Supplementary info for "Physics of Lumen growth"

Sabyasachi Dasgupta[a,b], **Kapish Gupta**[a], **Yue Zhang**[a], **Virgile Viasnoff**[a,c,d,1], **and Jacques Prost**[a,b]

[a]Mechanobiology Institute, National University of Singapore, Singapore 117411, Singapore; [b]Laboratoire Physico Chimie Curie, Institut Curie, PSL Research University, CNRS UMR168, 75005 Paris, France; [c]CNRS UMI3639, Singapore 117411, Singapore; [d]Department of Biological Sciences, National University of Singapore, Singapore 117411, Singapore

Supplementary info

SI(1): Hepatocyte culture conditions. Hepatocytes were isolated from male Wistar rats by *in situ* collagenase perfusion method. The animals were obtained from InVivos, Singapore. Animals were handled in accordance to the IACUC protocol approved by the IACUC committee of the National University of Singapore. Isolated hepatocytes were cultured in collagen sandwich for 48 hours. These cells were then treated with UDCA (20,40, 60, 80,100 µM) or Blebbistatin(1 µM) and imaged at a intervals of 90 seconds using an inverted wide-field fluorescence microscope (Nikon Biostation IMQ) for 3-4 hours.

SI(2): Justifications for orders of magnitude. In the numerical calculations we have used normalized units nu, such that $k_BT^{nu} = 1$ corresponds to $k_BT = 4.10^{-21}$ joule, $L^{nu} = 1$ corresponds to $L = 10^{-5}m$, and $t^{nu} = t/\tau$ such that $\Lambda_V^{nu} = 1$. This last choice implies τ values of a few $10^{11}s$ knowing that typical permeation coefficients are of the order of 10^{-11}m/Pa.s. Straightforward expressions follow for the normalized units of densities and osmotic pressures $\delta\rho^{nu} = L^3\delta\rho = \delta\pi^{nu}$. The pressure and surface tension units follow these rescaling in a simple way:$\delta P^{nu} = L^3\delta P/k_BT$ and $\sigma^{nu} = L^2\sigma/k_BT$. We have investigated reasonable parameters values. The choice of orders of magnitude of the screening length and the ion transport coefficient require some more analysis. From Eq.(4) one easily sees that $\Lambda = \Lambda_i k_BT\rho_{cell}$ has the dimension of a velocity. It is not easy to find experimental values of either Λ or Λ_i. However one finds easily conductivity values. If one recognizes that the real driving force is not the electric potential but the electrochemical potential, one can easily infer from conductivity data the values of Λ_i. One can infer $\Lambda \simeq 10^7ms^{-1}$ and hence $\Lambda^{nu} \simeq 10^9 - 10^{10}$. The estimate of $\xi_i^2 = Dw_0/2\Lambda$ follows immediately.Taking a reasonable value for an ion diffusion coefficient $D \simeq 10^{-10}m^2s^{-1}$ and $w_0 = 40$nm one obtains $\xi_i =$ a few microns and $\xi_i^{nu} =$ a few 10^{-1}. Last $\xi_V^2 = K_V/(2\Lambda_V)$; to our knowledge, there have been no measurement of K_V up to now. A purely hydrodynamic estimate would give $K_V = w_0^3/12\eta$ in which η is the fluid viscosity in the cleft. The difficulty here is to choose η. If we take hundred time that of water, which is of the order of the 'ill defined" plasma viscosity,and the already used order of magnitude for Λ one winds up with a fluid screening length again of the order of a few microns. Note that the uncertainty on the exact values of the parameters is not as bad as it seems since they come in a square root. As a consequence we have investigated ξ_V^{nu} in the 10^{-1} range. SI Appendix Table (S1) sums up the investigated domain range of the relevant parameters.

Now, we justify our approximation of a constant cleft thickness. We rewrite Eq (2) in a slightly different form:

$$\frac{\delta P}{k} = (e - e_0) - \xi_e^2\nabla^2 e\,, \qquad [1]$$

in which the length $\xi_e = \sqrt{\frac{\tilde\sigma}{k}}$ expresses the length scale over which thickness changes occur under localized solicitations. Whenever δP is comparable to the cell Laplace pressure, $e - e_0$ is of order $\frac{\tilde\sigma}{Lk}$. Taking $\tilde\sigma = afew10^{-4}nm^{-1}$ and $k = afew10^{12}nm^{-3}$ and $L = 10^{-5}m$ we find $e - e_0 =$ a few $10^{-11}m$ from which we deduce $\frac{e-e_0}{e_0}$ of order 10^{-3}. Thus the thickness of the cleft is close to the optimal thickness, up to a distance of order ξ_e from the lumen. This result holds in regions which are not subjected to localized forces. The same values of $\tilde\sigma$ and k lead to ξ_e of the order of the cleft thickness. Thus the approximation of constant thickness breaks down only at a nanoscopic scale, in the region where lumen and cleft merge.

Last we justify the local equilibrium approximation leading to the use of Eqs. (9) and (12) in the dynamical set of equations. The largest time for reaching local equilibrium ion density is $\tau_i = \frac{L^2}{D}$. With $L \simeq 10\mu m$ and $D \simeq 10^{-10}m^2s^{-1}$ we obtain $\tau_i \simeq .25s$. Similarly, the largest time for reaching local volume flux equilibrium is $\tau_V = \frac{L^2}{K_V k}$; with $L \simeq 10\mu m$, $K_V \simeq 10^{-22}m^3Pa^{-1}s^{-1}$ one obtains $\tau_V \simeq 1s$. Both times are significantly shorter than experimental times which are of the order of tens of minutes, hence the validity of Eqs. (9) and (12) in which r_l is a function of time.

SI(3): Analytical solutions of steady states in cleft. The solution to Eq.(9) reads:

$$\begin{aligned}\delta\rho(r) = \;& \frac{I_0(\frac{r}{\xi_i})\left[(\delta\rho_i - \delta\rho_{ext})K_0(\frac{r_l}{\xi_i}) + (\delta\rho_{lum} - \delta\rho_i)K_0(\frac{L}{\xi_i})\right]}{\left[K_0(\frac{L}{\xi_i})I_0(\frac{r_l}{\xi_i}) - I_0(\frac{L}{\xi_D})K_0(\frac{r_l}{\xi_i})\right]} \\ & + \frac{I_0(\frac{r_l}{\xi_i})\left[(\delta\rho_{ext} - \delta\rho_i)K_0(\frac{r}{\xi_i}) + \delta\rho_i K_0(\frac{L}{\xi_i})\right]}{\left[K_0(\frac{L}{\xi_i})I_0(\frac{r_l}{\xi_i}) - I_0(\frac{L}{\xi_i})K_0(\frac{r_l}{\xi_i})\right]} \\ & + \frac{I_0(\frac{L}{\xi_i})\left[(\delta\rho_i - \delta\rho_{lum})K_0(\frac{r}{\xi_i}) - \delta\rho_i K_0(\frac{r_l}{\xi_i})\right]}{\left[K_0(\frac{L}{\xi_i})I_0(\frac{r_l}{\xi_i}) - I_0(\frac{L}{\xi_i})K_0(\frac{r_l}{\xi_i})\right]}\,. \end{aligned} \qquad [2]$$

One can check directly that if the distance from any extremity is large compared to the screening length ξ_i, the value of the ion density is simply set by the source, i.e $\delta\rho(r) = \delta\rho_i$. The Bessel functions K_0 and I_0 can be thought of in a loose sense as generalizations of exponential functions for two dimensional laplacian problems; they do show exponential screening.

The solution to Eq.(12) has a similar structure:

$$\begin{aligned}
\delta P(r) =\ & \frac{K_0\left(\frac{r}{\xi_V}\right)\left(I_0\left(\frac{L}{\xi_V}\right)\left(\xi_V^2(\delta P - 2k_BT\delta\rho_i) - \xi_i^2(\delta P - 2k_BT\delta\rho)\right) + I_0\left(\frac{r_l}{\xi_V}\right)\left(\xi_i^2(\delta P_{ext} - 2k_BT\delta\rho_{ext}) - \xi_V^2(\delta P_{ext} - 2k_BT\delta\rho_i)\right)\right)}{(\xi_i - \xi_V)(\xi_i + \xi_V)\left(K_0\left(\frac{L}{\xi_V}\right) I_0\left(\frac{r_l}{\xi_V}\right) - I_0\left(\frac{L}{\xi_V}\right) K_0\left(\frac{r_l}{\xi_V}\right)\right)} \\
& + \frac{I_0\left(\frac{r}{\xi_V}\right)\left(K_0\left(\frac{L}{\xi_V}\right)\left(\xi_i^2(\delta P - 2k_BT\delta\rho) - \xi_V^2(\delta P - 2k_BT\delta\rho_i)\right) + K_0\left(\frac{r_l}{\xi_V}\right)\left(\xi_V^2(\delta P_{ext} - 2k_BT\delta\rho_i) - \xi_i^2(\delta P_{ext} - 2k_BT\delta\rho_{ext})\right)\right)}{(\xi_i - \xi_V)(\xi_i + \xi_V)\left(K_0\left(\frac{L}{\xi_V}\right) I_0\left(\frac{r_l}{\xi_V}\right) - I_0\left(\frac{L}{\xi_V}\right) K_0\left(\frac{r_l}{\xi_V}\right)\right)} \\
& + 2k_BT\left\{\frac{K_0\left(\frac{r}{\xi_i}\right)\left((\delta\rho_i - \delta\rho)I_0\left(\frac{L}{\xi_i}\right) + (\delta\rho_{ext} - \delta\rho_i)I_0\left(\frac{r_l}{\xi_i}\right)\right) + I_0\left(\frac{r}{\xi_i}\right)\left((\delta\rho - \delta\rho_i)K_0\left(\frac{L}{\xi_i}\right) + (\delta\rho_i - \delta\rho_{ext})K_0\left(\frac{r_l}{\xi_i}\right)\right)}{\left(1 - \frac{\xi_V^2}{\xi_i^2}\right)\left(K_0\left(\frac{L}{\xi_i}\right) I_0\left(\frac{r_l}{\xi_i}\right) - I_0\left(\frac{L}{\xi_i}\right) K_0\left(\frac{r_l}{\xi_i}\right)\right)} + \delta\rho_i\right\}
\end{aligned} \quad [3]$$

Even though, the expression is more complex than that of the ion density, it shares with it the feature that if the distance to boundaries is larger than both screening lengths ξ_i and ξ_V then the pressure is simply determined by the osmotic pressure corresponding to the excess ion density $\delta\rho_i$. Note that because the source term in Eq.(12) depends on space in a non trivial way, the two screening lengths play a role in this expression.

SI (4): derivation of the dynamical equations for lumen growth. We derive here the equations for the dynamics of the lumen growth with the variables R,θ, $\delta\rho$. For that, we must satisfy as explained in the main text, force balance and conservation laws, in the lumen and simultaneously in the paracellular domain.

The ion conservation Eq.(4) in the lumen is given by,

$$\begin{aligned}
\frac{dN}{dt} =\ & 2\pi R(t) \times \Lambda(2R(t)(1-\cos\theta(t))(\delta\rho_i - \delta\rho(t)) \\
& + \xi_i^2\left(\frac{\partial}{\partial r}\delta\rho(t)\right)\Big|_{r=r_l}\Big).
\end{aligned} \quad [4]$$

where $\Lambda = \frac{k_BT\Lambda_i}{\rho_{cell}}$. The total number of ions in the lumen is related to the lumen ion density by $N = V\rho = V(\rho_{cell} + \delta\rho)$. The geometrical relation $r_l(t) = R(t)\sin\theta(t)$ holds at any given time. In this expression the ion density gradient at the lumen-cleft interface is deduced directly from the derivative of the expression of $\delta\rho$ given by Eq. SI(2), taken at the value $r = r_l$. Indeed, according to the estimate given in section SI(2), the time dependent part of the cleft ion conseravtion Eq.(5) is completely negligible and one can use solutions of Eq.(9) with the slowly moving boundary $r_l(t)$.

The volume conservation Eq.(3) can be expressed in a similar way,

$$\begin{aligned}
\frac{dV}{dt} =\ & 2\pi R(t)\Lambda_v(2R(t)(1-\cos\theta(t))(2k_BT\delta\rho(t) \\
& - \tfrac{2\sigma(t)}{R(t)}) + \xi_V^2\left(\frac{\partial}{\partial r}\delta P\right)\Big|_{r=r_l}\Big).
\end{aligned} \quad [5]$$

The volume is easily expressed in terms of the lumen radius of curvature $R(t)$ by $V = \frac{\pi}{3}R(t)^3(1-\cos\theta(t))^2(2+\cos\theta(t))$. The pressure gradient at the lumen-cleft interface is deduced from the derivative of expression Eq. SI(3) taken at $r = r_l$. Indeed as for the ion density equation, the time derivative part of the volume conservation equation can be safely neglected and Eq.(12) derived from Eq.(4) holds at all times.

We can then solve Eq. (3), Eq. SI(4) and Eq. SI(5) with the dynamical tension given by Eq.(15), to obtain $R(t)$, $\delta\rho(t)$ and $\theta(t)$ provided we specify the initial conditions $R(t=0)$, $\delta\rho(t=0)$ and $\theta(t=0)$.

SI(5): Analytical solutions of dynamical equations in the large lumen limit.. We discuss here the limit of large lumens ($L - r_l << \xi_i$, $L - r_l << \xi_V$) with small deviations from steady state values of the variables $R, \theta, \delta\rho$, in which it is possible to derive an analytical solution . In this regime, the leaks take the simple form $\left(\frac{\partial}{\partial r}\delta P\right)\Big|_{r=r_l} \approx -\frac{(P-P_{ext})}{L-r_l}$, and $\left(\frac{\partial}{\partial r}\delta\rho\right)\Big|_{r=r_l} \approx -\frac{(\delta\rho-\delta\rho_{ext})}{L-r_l}$, and the dynamical equations can be linearized. A further simplification is obtained by anticipating that the Laplace pressure is small compared to the osmotic pressure and thus can be neglected in the water conservation equation. Looking for exponentially relaxing quantities $O(t) - O_s = \tilde{O}\exp st$, where $O(t)$ is any of the system variable, the compatibility requirement of the system of dynamical equations provides a simple second order equation $ax^2 + bx + c = 0$ for the reduced variable $x = \tau_c s$. The expressions for a, b, and c can be obtained analytically and read when $\delta\rho_{ext} = 0$, $\delta P_{ext} = 0$:

$$\begin{aligned}
a \simeq\ & \tfrac{\cos\theta_s}{2(1+\cos\theta_s)^2}\left(\tfrac{1}{\Lambda_V} + \tfrac{k_BT\rho_{cell}}{\Lambda}\right) \\
& + \tfrac{\cos\theta_s\xi_i}{2\Lambda_V\xi_V(1+\cos\theta_s)^2}\sqrt{\tfrac{k\delta\rho_iL}{\sigma_0\sin\theta_s}}
\end{aligned} \quad [6]$$

$$b \simeq \frac{2-\cos\theta_s-\cos\theta_s^2}{\cos\theta_s}\left(\frac{k_B T\rho_{cell}}{\Lambda(1+\cos\theta_s)}+\frac{\xi_i}{2\Lambda_V\xi_V\sin\theta_s^2)}\sqrt{\frac{k_B T\delta\rho_i L}{\sigma_0\sin\theta_s}}\right) - \left(\frac{\tau_c L(1-\cos\theta_s)(k_B T\delta\rho_i)^{3/2}}{(1+\cos\theta_s)^3\sin\theta_s\xi_i\xi_V(\sigma_0\sin\theta_s/L)^{1/2}}\right) \tag{7}$$

$$c \simeq \frac{2\tau_c L\tan\theta_s}{\xi_i\xi_V(1+\cos\theta_s)^3}\frac{(k_B T\delta\rho_i)^{3/2}}{(\sigma_0\sin\theta_s/L)^{1/2}} \tag{8}$$

For small enough Λ_v,Λ, and $\delta\rho_i$ the three coefficents a, b, c and the discriminant $b^2 - 4ac$ are positive. Furthermore $\sqrt{b^2 - 4ac}$ is smaller than b and the two roots of the x equation are negative: the system relaxes monotonously to steady state in the linear regime. This regime is overdamped. Upon increasing any of the three parameters Λ_V,Λ, and $\delta\rho_i$ the system gets into a regime in which the discriminant $b^2 - 4ac$ of the equation becomes negative, while a, b, c are still positive. The two roots of the x equation are complex conjugate with a negative real part. The system relaxes to steady state, with oscillations of decreasing amplitude as time goes on. This is an underdamped regime. Upon increasing even more λ_w,λ_N, or $\delta\rho_i$ the system reaches a point where $b = 0$. At that point the roots are pure imaginary and beyond the real part becomes positive, meaning that any fluctuation is amplified at the frequency defined by the imaginary part of x.This defines a Hopf bifurcation. The complete numerical solution confirms this scenario as already observed. Note that the feedback from the cortex viscosity is essential in obtaining the spontaneous oscillations which are being observed in a physiologically relevant domain of parameter space. Supplementary Films 2-4 display animations of the lumen dynamics in the different growth scenario. We give on Fig. 1 an example of phase diagram in a $\delta\rho_i$,Λ plane for prescribed Λ_V based on the analytical expressions above. One clearly sees the independence of Λ for large values and the succession of the overdamped, underdamped, oscillatory regimes for increasing $\delta\rho_i$. The agreement of the analytic expression of the Hopf phase boundary and the overdamped-underdamped regimes cross-over with the numerical calculation is qualitative since, the approximate expression of the leaks does not hold true in general, for the physically relevant values of $\delta\rho_i$ where we have presented the full solution of the dynamics using numerical methods.

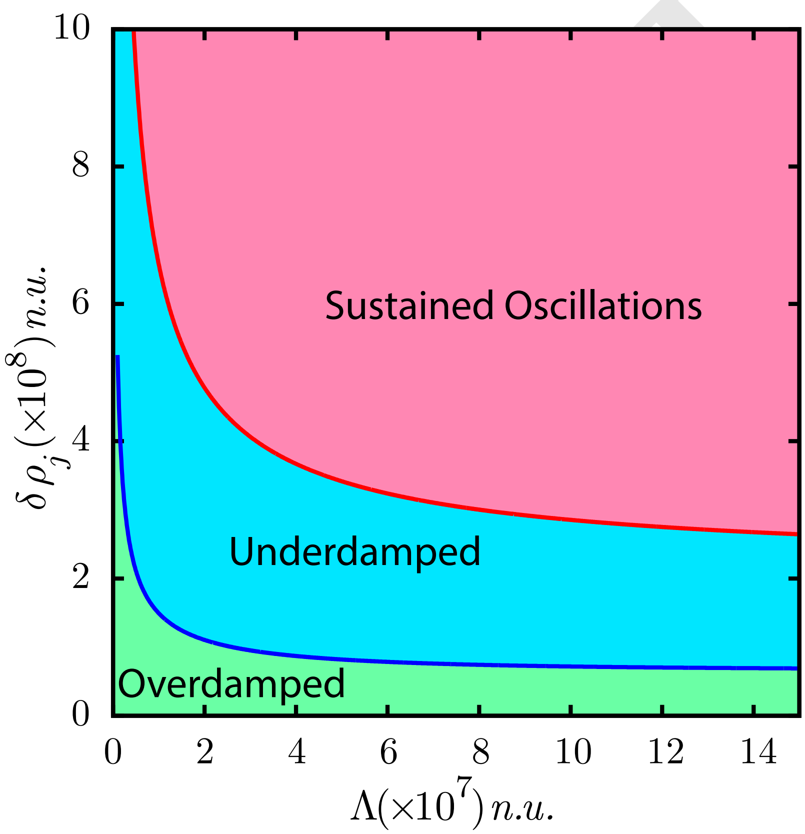

Fig. 1. Dynamical state diagram of the cell-lumen system in a $\delta\rho_i$ - Λ plane, as obtained from the analytical estimate of SI (5) for $\xi_V = 0.49$, $\xi_i = 0.50$, $\Lambda_v = 1$ *n.u.*, $\sigma_0 = 10^7$ *n.u.*, $\delta\rho_{ext} = -2 \times 10^6$ *n.u.*, and $\rho_{cell} = 10^9$ *n.u.*.

Tables

Input parameters	Definition	Estimated values	Normalized units
k_BT	Boltzmann factor	4.1 pN-nM	1 *n.u.*
L	Lateral size of cell	10 μm range	1 *n.u.*
R	Radius of curvature of lumen	10 μm range	~ 1 *n.u.*
r_l	Position of lumen junction with the cleft in polar co-ordinates	μm range	~ 1 *n.u.*
$\theta, (\theta_s)$	Angle, (steady state angle) between the tangent to the lumen at r_l, and the symmetry plane	0 , $\pi/2$ range	0 , $\pi/2$ range
Λ_V	Water permeation coefficient	$\sim 10^{-10} - 10^{-11}$ $m^3/(Ns)$	~ 1
Λ	Ion permeation coefficient	$\sim 10^{-9} - 10^{-7}$ m/s	$\sim 10^7 - 10^{10}$
$\delta\rho_i$	Total ion density difference between lumen and cell such that passive and active fluxes balance as the measure of secretory efficiency of the membrane.	$\sim$ 0.1 -10 mM	$\sim 10^8 - 10^{10}$
$\delta\rho_{ext}$	Ion density outside the cell minus cell ion density	$\sim$-(0.1 -1) mM	$\sim (-10^7)$
σ_0	Sum of cortex and membrane tension in the lumen at steady state	$\sim 10^{-4}$ N/m	$\sim 10^7$
$\tilde{\sigma}_0$	Sum of cortex and membrane tension in the cleft minus the cell-cell adhesion energy E	$\sim 10^{-4}$ N/m	$\sim 10^7$
ξ_i	Characteristic length scale the ion leak in the cleft	μm range	$\sim$ 0.1-0.5
ξ_V	Characteristic length scale the water leak in the cleft	μm range	$\sim$ 0.1-0.5
τ_c	Cortex crossover time	$\sim 10^2 - 10^4$ s	$\sim 10^{-8} - 10^{-9}$

Table 1. Estimation of the values of Physical parameters for cell-cell interface lumen formation model

$\delta\rho_i$	r_0^u	R^u	r_l^{ini}	R^{ini}
1.0×10^8	0.248745	0.497489	0.251232	0.502464
1.35×10^8	0.161707	0.323414	0.163324	0.326648
1.38×10^8	0.158089	0.316179	0.159670	0.319340

Table 2. Initial values of r_o^{ini}, R^{ini} for obtaining numerical solution of dynamical behavior in Fig. 3 and Fig. 4. The values are obtained by estimating first the value of R^u and r_0^u at the unstable branch at the same $\delta\rho_i$ and then initial values are used as 1$\%$ more than the value at the unstable branch.

Legends for SI movies

The SI movies exemplify the dynamics of lumen growth in the 3 different regimes obtained from our model

Movie 1: Animation of the lumen growth dynamics in the monotonous growth regime.Volume, ion density as well as the lumen shapes are presented. Note that the concentration of the lumen is coded by different intensity of green color.The simulation parameters are the same as in the main text.

Movie 2: Animation of the lumen growth dynamics in the sustained oscillation regime.Volume, ion density as well as the lumen shapes are presented. Note that the concentration of the lumen is coded by different intensity of green color.The simulation parameters are the same as in the main text.

Movie 3: Animation of the lumen growth dynamics in the damped oscillation regime.Volume, ion density as well as the lumen shapes are presented. Note that the concentration of the lumen is coded by different intensity of green color. The simulation parameters are the same as in the main text.